High-spin Ni3Fe2(CN)(6) and Cu3Cr2(CN)(6) clusters based on a trigonal bipyramidal geometry

ARTICLE *in* ZEITSCHRIFT FÜR ANORGANISCHE CHEMIE · OCTOBER 2007

Impact Factor: 1.16 · DOI: 10.1002/zaac.200700273

4 AUTHORS, INCLUDING:

Bart M Bartlett
University of Michigan
61 PUBLICATIONS **2,385** CITATIONS
SEE PROFILE

M.W. Degroot
Dow Chemical Company
22 PUBLICATIONS **342** CITATIONS
SEE PROFILE

DOI: 10.1002/zaac.200700273

High-Spin $Ni_3Fe_2(CN)_6$ and $Cu_3Cr_2(CN)_6$ Clusters Based on a Trigonal Bipyramidal Geometry

Bart M. Bartlett, T. David Harris, Marty W. DeGroot, and Jeffrey R. Long*

Berkeley, CA / USA, University of California, Department of Chemistry

Received April 21st, 2007.

Dedicated to Professor Dieter Fenske on the Occasion of his 65th Birthday

Abstract. The synthesis and characterization of two new cyano-bridged cluster compounds, $[Tp_2(cyclen)_3Ni^{II}_3Fe^{III}_2(CN)_6](BF_4)_4$ (**1**) and $[(Me_3tacn)_5Cu^{II}_3Cr^{III}_2(CN)_6](ClO_4)_6$ (**2**), are reported. The structure of each cluster is based upon a trigonal bipyramidal geometry, and ferromagnetic coupling between constituent metal ions is shown to give rise to $S = 4$ and $S = {}^9/_2$ ground states, respectively. A room-temperature assembly reaction generates a purple form of compound **2**, wherein two cyanide stretching frequencies in the infrared spectrum (ν_{CN} = 2094, 2156 cm^{-1}) indicate partial isomerism of the cyanide bridging ligands. The X-ray crystal structure confirms this isomerism via examination of the C and N thermal parameters. At −40 °C, a metastable green form of the compound is instead isolated, for which a single cyanide stretch at ν_{CN} = 2156 cm^{-1} is consistent with an unisomerized cluster. The temperature-dependence of the magnetization under varying applied field reveals significant axial anisotropy in compound **1**, with a significant axial zero-field splitting while compound **2** shows no zero-field splitting in either isolated form. In line with the observed anisotropy, AC magnetic susceptibility measurements performed on compound **1** reveal a frequency-dependent out-of-phase signal suggestive of single-molecule magnet behavior.

Keywords: Magnetic properties; Cluster compounds; Cyanides; Single-molecule magnets; Trigonal bipyramid

Introduction

Since the discovery that $[Mn_{12}O_{12}(CH_3CO_2)_{16}(H_2O)_4]$ exhibits magnetic bistability associated with its $S = 10$ ground state [1], there has been much interest in developing new single-molecule magnets for potential applications in information storage and quantum computing [2]. Despite the synthesis of many new species showing similar behavior, the highest spin-reversal barrier encountered to date is just 60 cm^{-1} [3], only a modest increase over that of the original cluster. The spin-reversal barrier for a single-molecule magnet with total spin S and axial anisotropy D is given by $S^2|D|$ for molecules with integer values of S and $(S^2 - {}^1/_4)|D|$ for half-integer values of S. While the record for the spin ground state of a molecule is currently ${}^{83}/_2$ [4], predictability and control of anisotropy remains an important challenge in the rational design of new single-molecule magnets with enhanced blocking temperatures.

Understanding anisotropy arising from the zero-field splitting in the ground state is a focus of current efforts in our laboratory. The experimentally measured axial anisotropy is governed by two factors − that arising from the single-ion anisotropy of each constituent metal ion and that dictated by the overall distribution of electrons in the molecule. In order to deconvolute the two sources, our research has taken advantage of cyanide as a bridging ligand, which can sometimes allow for predictable molecular geometries and adjustable magnetic properties [5].

There have been several recent reports on the magnetic properties of trigonal bipyramidal cyano-bridged clusters featuring first-row transition metals accompanied by a variety of ancillary ligands on the metals in the equatorial positions [6]. We note, however, that many of these molecules possess terminal cyanide ligands in the axial positions, which can give rise to intermolecular magnetic exchange interactions via hydrogen-bonding. While not observed in all such clusters, long-range magnetic ordering is indeed evident for the compounds $[(Ni(bpm)_2)_3(Fe(CN)_6)_2]\cdot 7H_2O$ (bpm = bis(1-pyrazolyl)methane), $[(Ni(2,2'\text{-bpy})_2)_3(Fe(CN)_6)_2]\cdot 13H_2O$, and $[(Cu(2,2'\text{-bpy})_2)_3(Fe(CN)_6)_2]\cdot 10H_2O$ [6a,b]. Additionally, *Zuo* and coworkers have prepared trigonal bipyramidal clusters with $[TpFe(CN)_3]^-$ (Tp^- = hydrotris(1-pyrazolyl)borate) complexes in the equatorial positions, again leaving terminal cyanide ligands [6e].

Recently, a trigonal bipyramidal cluster with no terminal cyanide ligands, $[Tp_2(Me_3tacn)_3Cu_3Fe_2(CN)_6]^{4+}$ (Me_3tacn = 1,4,7-trimethyl-1,4,7-triazacyclononane), was reported to

* Prof. Jeffrey R. Long
Department of Chemistry
University of California
Berkeley, CA 94709-1460 USA
Fax: (+) 1-510-642-8369
E-mail: jrlong@berkeley.edu

Supporting information for this article is available on the WWW under **http://www.wiley-vch.de/home/zaac** or from the author

show single-molecule-magnet behavior arising from an $S = {}^5/_2$ ground state with a remarkably large axial zero-field splitting of $D = -5.7\ cm^{-1}$ [7]. We therefore sought to prepare other, higher-spin clusters based on a similar fully-terminated trigonal bipyramidal geometry. Toward that end, we herein report the synthesis and magnetic properties of $[Tp_2(cyclen)_3Ni_3Fe_2(CN)_6](BF_4)_4$ (**1**; cyclen = 1,4,7,10-tetraazacyclododecane) and $[(Me_3tacn)_5Cu_3Cr_2(CN)_6](ClO_4)_6$ (**2**; Me_3tacn = *N,N′,N″*-trimethyl-1,4,7-triazacyclononane).

Experimental Section

General Considerations

All reagents except for Me_3tacn were purchased from commerical vendors and used as received. Me_3tacn was obtained from Unilever, and distilled under vacuum (36 °C at ca. 80 mTorr) prior to use. Acetonitrile and diethyl ether were dried over activated alumina, and absolute ethanol was distilled over Mg/I_2 prior to use. The compounds $[Bu_4N][TpFe(CN)_3]$ [8], $[(Me_3tacn)Cr(CN)_3]$ [9], and $[(Me_3tacn)Cu(H_2O)_2](ClO_4)_2$ [10] were prepared as previously described. The compound $[Ni(cyclen)](BF_4)_2$ was prepared in a manner analogous to that previously reported for the ClO_4^- salt [11]. Infrared spectra were recorded on a Nicolet AVATAR 350 FT-IR spectrometer equipped with a SMART MIRacle ZnSe ATR accessory, and electronic absorption spectra were recorded on a Hewlett-Packard 845X UV-vis spectrophotometer. Mass spectra were acquired on a Waters "Q-TOF Premier" quadrupole time-of-flight mass spectrometer equipped with an electrospray ionization (ESI) source. Chemical analyses (C, H, and N) were performed at U.C. Berkeley College of Chemistry Microanalytical Laboratory.

Synthesis of $[Tp_2(cyclen)_3Ni_3Fe_2(CN)_6](BF_4)_4{\cdot}4H_2O$ (1)

A 15-mL 2:1 EtOH:MeCN solution containing 0.208 g of $[Ni(cyclen)](BF_4)_2$ (0.514 mmol) was added dropwise to a 15-mL CH_3CN solution containing 0.197 g of $[Bu_4N][TpFe(CN)_3]$ (0.334 mmol) to give a homogeneous orange-red solution. The reaction mixture was stirred for approximately 15 min, and red block-shaped crystals suitable for X-ray structure determination and magnetic measurements were obtained from vapor diffusion of Et_2O under ambient conditions. Crystalline yield: 0.199 g (0.104 mmol, 63 % based on starting $[TpFe(CN)_3]^-$). IR (ATR) ν(CN) 2160 cm^{-1}. Anal. Calcd. for $C_{48}H_{89}B_6F_{16}Fe_2N_{30}Ni_3O_{4.5}$: C, 31.76; H, 4.94; N, 23.15. Found: C, 32.37; H, 5.15; N, 22.88 %.

Synthesis of Partially-Isomerized $[(Me_3tacn)_5Cu_3Cr_2(CN)_6](ClO_4)_6{\cdot}5CH_3CN$ (2β)

A 2-mL EtOH solution containing 0.070 g of $[(Me_3tacn)Cu(H_2O)_2](ClO_4)_2$ (0.15 mmol) was added dropwise to a 3-mL CH_3CN suspension containing 0.029 g of $[(Me_3tacn)Cr(CN)_3]$ (0.33 mmol) to give an immediate green solution that gradually turned dark purple over the course of 1 h. Purple plate-shaped crystals suitable for X-ray structure determination and magnetic measurements were obtained from vapor diffusion of Et_2O. Crystalline yield: 0.068 g (0.036 mmol, 74 %). IR (ATR) ν(CN) 2094, 2156 cm^{-1}. Anal. Calcd. for $C_{51}H_{105}Cl_6Cr_2Cu_3N_{21}O_{24}$: C, 32.17; H, 5.56; N, 15.45. Found: C, 31.95; H, 5.76; N, 15.43 %.

Synthesis of Unisomerized $[(Me_3tacn)_5Cu_3Cr_2(CN)_6](ClO_4)_6$ (2α)

A 2-mL EtOH solution containing 0.025 g of $[(Me_3tacn)Cu(H_2O)_2](ClO_4)_2$ (0.083 mmol) and a 3-mL CH_3CN suspension containing 0.058 g of $[(Me_3tacn)Cr(CN)_3]$ (0.12 mmol) were cooled to −40 °C in separate test tubes. The solution containing $[(Me_3tacn)Cu(H_2O)_2](ClO_4)_2$ was then added dropwise to the suspension containing $[(Me_3tacn)Cr(CN)_3]$ with stirring to give a green solution. After stirring for 10 min at −40 °C, the solution was filtered through Celite. Diffusion of Et_2O vapor into the green filtrate at −25 °C precipitated a green, microcrystalline solid. The solid was collected via filtration and washed with Et_2O (2 × 1 mL). Yield: 0.057 g (0.030 mmol, 72 %). IR (ATR): ν(CN) 2156 cm^{-1}. ESI-MS$^+$: m/z = 1803 ($[M(ClO_4)_5]^+$).

X-Ray Crystallography

X-Ray Structure Determinations. Structures were determined for the compounds listed in Table 1. Single crystals were picked from the reaction mixtures, coated with Paratone-N oil, attached to Kaptan loops, and transferred to the diffractometer under a cold stream of nitrogen. Initial lattice parameters were obtained from a least-squares analysis of at least 80 reflections; these parameters were later refined against all data. Data were integrated and corrected for Lorentz and polarization effects with SAINT+ 6.22 and were corrected for absorption effects with SADABS 2.03.

Table 1 X-ray crystallographic data for **1** and **2**.[a)]

	Ni_3Fe_2 (**1**)	Cu_3Cr_2 (**2β**)
Empirical Formula	$C_{48}H_{89}B_6F_{16}Fe_2N_{30}Ni_3O_{4.5}$	$C_{61}H_{120}Cl_6Cr_2Cu_3N_{26}O_{24}$
Formula Weight	1815.03	2109.11
Temperature /K	148(2)	153(2)
Wavelength /Å	0.71073	0.71073
Crystal system	cubic	triclinic
Space group	$I\bar{4}3m$	$P\bar{1}$
Unit cell dimensions /Å	a = 26.415(3)	a = 14.798(3) b = 15.465(3) c = 22.660(5)
Unit cell angles /deg	α = 90	α = 88.18(3) β = 81.37(3) γ = 64.63(3)
Volume /Å^3, Z	18431(4), 8	4629.4(16), 2
$\rho_{calc'd}$	1.261	1.513
Abs. Coeff. /mm^{-1}	0.989	1.159
F(000)	7168	2194
Crystal size /mm	0.30 × 0.15 × 0.07	0.22 × 0.20 × 0.08
θ range /deg	1.89 − 23.29	4.39 − 37.91
Reflections collected	42224	18783
Unique Reflections	2460 [R_{int} = 0.0621]	9642 [R_{int} = 0.0536]
Completeness to θ	99.8 %	99.1 %
Absorption correction		Semi-empirical from equivalents
Refinement method		Full matrix least-squares on F^2
Data / restraints / parameters	2460 / 0 / 206	9642 / 0 / 1021
GoF on F^2	1.272	1.036
Final R indices	$R1$ = 0.0678	$R1$ = 0.0670
[$I > 2\sigma(I)$]	$wR2$ = 0.1869	$wR2$ = 0.1683
R indices (all data)	$R1$ = 0.0770 $wR2$ = 0.1980	$R1$ = 0.1112 $wR2$ = 0.1852

[a)] Crystallographic data for these structures have been deposited with the Cambridge Crystallographic Data Centre (646856 and 646857), and can be obtained free of charge from the CCDC via www.ccdc.cam.ac.uk/data_request/cif.

Space group assignments were based on systematic absences, *E*-statistics, and successful refinement of the structures. Structures were solved by direct methods with the aid of successive difference Fourier maps, and were refined against all data using the SHELXTL 6.10 software package. Thermal parameters for all non-hydrogen atoms were refined anisotropically. Hydrogen atoms of organic ligands were assigned to ideal positions and refined using a riding model with an isotropic thermal parameter 1.2 times that of the attached carbon or nitrogen atoms.

Magnetic Measurements

Samples were prepared as finely ground powders in a frozen eicosane matrix and contained within polycarbonate capsules. Magnetic susceptibility measurements were performed using a Quantum Design MPMS2 SQUID magnetometer. DC susceptibility data were recorded at temperatures ranging from 5 to 300 K under an applied field of 1 kOe. Magnetization measurements were performed at temperatures ranging from 1.7 to 10 K, employing applied fields from 1 to 7 T at 1 T intervals. AC susceptibility data for compound **1** were recorded under an applied field $H = H_{ac}\sin(\omega t)$ where H_{ac}, the amplitude of the oscillating field was 4 Oe, and ω, the driving frequency, was varied from 50 to 1500 Hz. All data were corrected for diamagnetic contributions from the sample holder and eicosane, as well as for the core diamagnetism of each sample (estimated using Pascal's constants).

Results and Discussion

Synthesis and Structural Characterization

Both **1** and **2** were prepared via direct molecular self-assembly using a building-block approach. Three-fold symmetry was enforced by blocking off one face of the metal ions in the axial positions using the tridentate ligands Tp^- in **1** and Me_3tacn in **2**, with the other three coordination sites occupied by the cyanide bridging-ligand. Then, in order to obtain the trigonal bipyramids, the cis-directing ligand 1,4,7,10-tetraazacyclododecane (cyclen) was used for the octahedral Ni^{2+} ion in compound **1**, while Me_3tacn was employed to cap the square pyramidal Cu^{2+} ion in compound **2**. Both cluster-containing products are highly soluble in polar organic solvents, and are readily crystallized from vapor diffusion of diethyl ether.

X-ray crystal data and structural refinement parameters of compounds **1** and **2** are presented in Table 1. Compound **1** crystallizes in the cubic space group $I\bar{4}3m$, with a unit cell composed of eight formula units, one in each octant of the cube, with the local *z*-axis of each trigonal bipyramid residing on the crystallographic 3-fold axis. As shown in Figure 1, the cyanide bridging ligand enforces a nearly linear Fe−C≡N−Ni geometry, with mean Fe−C≡N and Ni−N≡C angles of 178.9(6)° and 172(5)°, respectively. The mean Fe−C distance of 1.93(2) Å is similar to that of the $[TpFe(CN)_3]^-$ precursor complex, supporting the structural model of the carbon end of cyanide bound to iron. In the high-symmetry structure, only two of the BF_4^- counteranions could be located in the difference Fourier map. The fluorine atoms of the other two anions were assigned the positions of highest residual electron density from the Fourier map and refined anisotropically. These fluorine atoms are highly disordered, and the boron atoms could not be located.

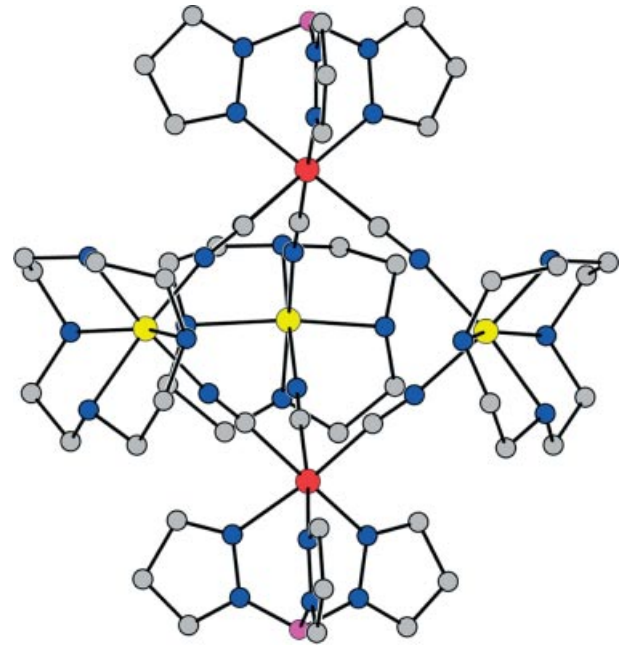

Figure 1 Structure of the trigonal bipyramidal cluster $[Tp_2(cyclen)_3Ni_3Fe_2(CN)_6]^{4+}$, as observed in **1**. Red, yellow, magenta, gray, and blue spheres represent Fe, Ni, B, C, and N atoms, respectively; H atoms are omitted for clarity.

The crystal structure of **2β** reveals an analogous trigonal bipyramidal core geometry, as depicted in Figure 2. The formation of this compound, however, involves a thermally-

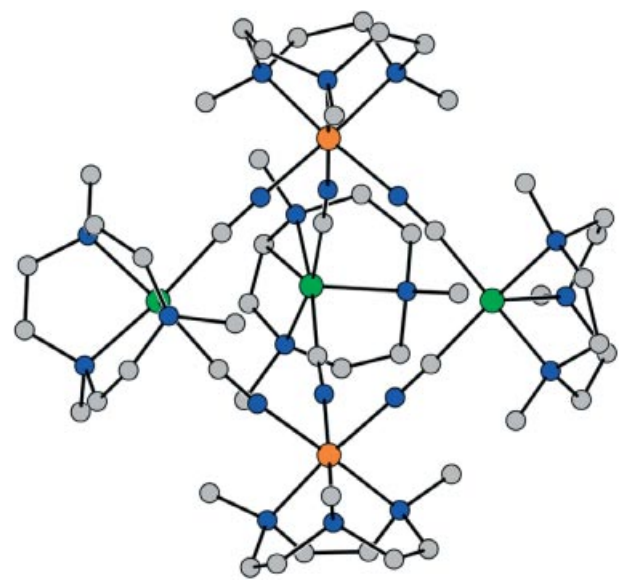

Figure 2 Structure of the trigonal bipyramidal cluster $[(Me_3tacn)_5Cu_3Cr_2(CN)_6]^{6+}$, as observed in **2β**. Orange, green, gray, and blue spheres represent Cr, Cu, C, and N atoms, respectively; H atoms are omitted for clarity.

induced linkage isomerism, wherein the cyanide ligands reorient such that their carbon and nitrogen atoms ligate the Cu^{II} and Cr^{III} atoms, respectively. This isomerism became evident in a comparison of thermal parameters in the X-ray structure of **2β** (where β denotes the cluster with cyanide isomerism, and α, the unisomerized cluster). Refining the structure as having all Cr−C≡N−Cu linkages led to non-positive definite thermal parameters for all six cyanide carbon atoms and thermal parameters in the range 0.017−0.12 $Å^2$ for the nitrogen atoms. In contrast, reorientation of the cyanides, followed by refinement, gave carbon thermal parameters in the range 0.015−0.032 $Å^2$ and nitrogen thermal parameters in the range 0.017−0.042 $Å^2$. While the thermal parameters resulting from all Cr−N≡C−Cu linkages are significantly better-behaved than those from all Cr−C≡N−Cu linkages, the low values of the former suggest that the crystal contains both linkages. To probe the possibility of partial isomerism, the data were modeled with the cyanide carbon and nitrogen site occupancies allowed to freely refine. This model gives a free variable value of 0.98(6), meaning the single crystal is 92−100 % isomerized. This value can only be considered as an estimate, however, as the scattering factors of carbon and nitrogen are very similar. Furthermore, the identical Cr−N≡C and Cu−C≡N bond angles of 174(1)° did not readily distinguish between the carbon and nitrogen positions of the cyanide bridging ligands.

Further evidence for cyanide ligand reorientation was obtained from the infrared spectrum of **2β**. Two distinct stretches of similar intensity are observed in the cyanide stretching region at 2094 and 2156 cm^{-1}, corresponding to the Cr−N≡C−Cu and Cr−C≡N−Cu linkages, respectively. While the presence of both peaks indicates that the product is partially isomerized, the extent of isomerism cannot be accurately quantified from these data, since the extinction coefficients of the peaks for two linkages are not necessarily equal. Thermodynamics likely drives the reorientation, with the softer carbon end of cyanide preferring the softer Cu^{II} atom over the harder Cr^{III} atom. Numerous instances of such cyanide linkage isomerism have now been observed in both extended solids [12] and molecular species [13], including the face-centered cubic cluster $[Tp_8(H_2O)_6Cu_6Cr_8(CN)_{24}]^{4+}$ reported recently [13b].

In an attempt to isolate the kinetically-favored isomer of the Cu_3Cr_2 cluster, the reaction between $[(Me_3tacn)Cr(CN)_3]$ and $[(Me_3tacn)Cu(H_2O)_2](ClO_4)_2$ was conducted at −40 °C. Diffusion of diethyl ether vapor into the resulting green solution at −25 °C produced a green, microcrystalline solid, with an infrared spectrum displaying a single cyanide stretch at 2156 cm^{-1}, consistent with unisomerized $[(Me_3tacn)_5Cu_3Cr_2(CN)_6](ClO_4)_6$ (**2α**). When heated at 90 °C, a solid sample of **2α** gradually changes from green to purple over the course of 8 h. When the temperature is increased to 120 °C, the solid ultimately turns orange. Time-resolved infrared spectra associated with these changes are shown in the left panel of Figure 3, where the original peak at 2156 cm^{-1} gradually disappears, and a new peak at 2096 cm^{-1} emerges.The spectrum recorded at 8 h is similar to that of the independently prepared sample of 2**β** (showing cyanide stretches at 2094 and 2156 cm^{-1}). The spectral changes occur rapidly for the first 8 h of heating, then slow considerably, with complete loss of the original peak occurring only after 62 h. During the final 18 h of heating, as the sample becomes orange, a new peak of low intensity appears at 2222 cm^{-1}. This peak likely corresponds to a cluster decomposition product.

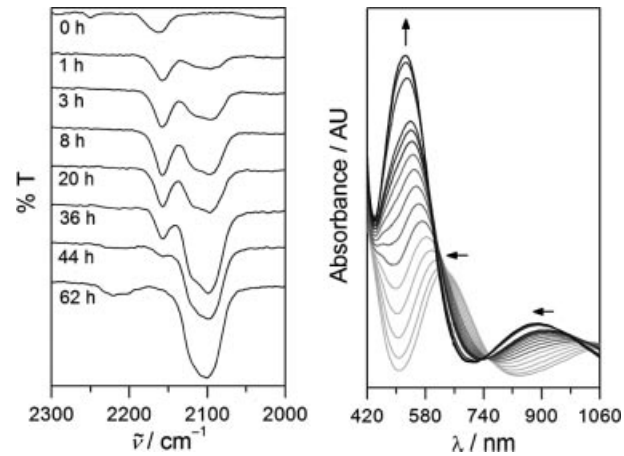

Figure 3 Left: Time-resolved infrared spectra for a pulverized sample of **2α**. The sample was heated for 30 h at 90 °C, followed by 32 h at 120 °C. Right: UV-visible absorption spectra of a room-temperature solution of 2α in a 3:2 mixture of acetonitrile and ethanol. Spectra were collected at 5 min intervals during the first hour, then at 2 h intervals during the following 6 h. Arrows indicate the direction of peak shifts with time.

Time-resolved UV-vis absorption spectra collected for a solution of **2α** at room temperature are shown on the right panel of Figure 3. Similar to the color change observed in the solid, the solution also changes from green to purple, although at a much faster rate. Over the course of 8 h, a peak at 632 nm increases in intensity and undergoes a hypsochromic shift to 523 nm, and a lower energy peak shifts to 891 nm. The lack of clean isosbestic points in the spectra suggests that the isomerism does not proceed through a synchronous reorientation of all six cyanides. Rather, the reaction path likely involves cluster molecules displaying varying degrees of isomerism.

Magnetic Properties

The magnetism of clusters **1** and **2** was investigated through DC susceptibility measurements in an applied field of 1 kOe. As illustrated in Figure 4, the room-temperature susceptibility for compound **1** gives $\chi_M T$ = 4.90 emu·K/mol, slightly higher than the expected product of 3.75 emu·K/mol predicted in the absence of exchange coupling with a Landé *g*-factor of 2.00. With decreasing temperature, $\chi_M T$ rises to a maximum value of 10.42 emu·K/mol at 5 K, consistent with the expected ferromagnetic coupling between low-spin Fe^{III} and Ni^{II} to give an S = 4 ground state. Below 5 K,

$\chi_M T$ drops sharply to a value of 9.48 emu·K/mol at 1.8 K, suggesting the presence of zero-field splitting in the ground state. The data above 5 K were fit using MAGFIT 3.1 [14] and the Heisenberg-van Vleck-Dirac Hamiltonian $\hat{H} = -2J\,[(\hat{S}_{M1} + \hat{S}_{M2})\cdot(\hat{S}_{M'1} + \hat{S}_{M'2} + \hat{S}_{M'3})]$, where M = Fe and M′ = Ni. The results gave $J = +5.4\,cm^{-1}$ and $g = 2.21$, with a temperature-independent paramagnetism contribution of $500 \times 10^{-6}\,cm^{-1}$. Note that the observed exchange coupling is very similar to the value of $J = +4.8\,cm^{-1}$ obtained for the related trigonal bipyramidal cluster $[(Tpm^{Me2})_2Tp_3Fe_3Ni_2(\mu\text{-}CN)_6(CN)_3]^+$ [6e].

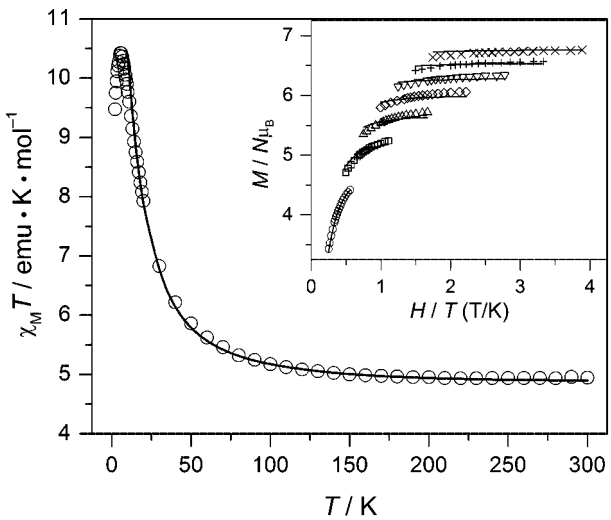

Figure 4 Temperature-dependence of the DC magnetic susceptibility data for compound **1**. The solid line represents the fit to the spin Hamiltonian described in the text. Inset. Reduced magnetization data for 1 in applied fields of 1 T (○) to 7 T (×) (in 1 T intervals), showing non-superimposable lines, indicating the presence of zero-field splitting. The solid lines represent fits to the zero-field splitting Hamiltonian described in reference [15].

Magnetization data for compound **1** collected between 1.8 and 4 K provides further evidence of zero-field splitting in the ground state. Fitting the non-superimposed isofield lines using ANISOFIT 2.0 [15] afforded two reasonable solutions − one with axial and transverse zero-field splitting parameters of $D = -1.7\,cm^{-1}$ and $E = 0.02\,cm^{-1}$, respectively and $g = 2.16$, and one with $D = 2.6\,cm^{-1}$, $E = 0.18\,cm^{-1}$, and $g = 2.15$. The latter solution gives a slightly better fit to the experimental data, and is shown in the inset of Figure 4. We note, however, that in a powder measurement it is often difficult to establish the sign of *D*. Regardless, the zero-field splitting parameter associated with the $S = 4$ ground state of $[Tp_2(cyclen)_3Ni_3Fe_2\text{-}(CN)_6]^{4+}$ is large in magnitude, although reduced relative to the $-5.7\,cm^{-1}$ observed for the closely-related trigonal bipyramidal cluster $[Tp_2(Me_3tacn)_3Cu_3Fe_2(CN)_6]^{4+}$ [7].

To probe the possible existence of magnetic bistability, AC magnetic susceptibility measurements were performed on **1**. As shown in Figure 5, a frequency-dependent signal is observed for the out-of-phase susceptibility, χ'', indicating the onset of slow magnetic relaxation at very low temperatures. The results suggest that *D* is actually negative for the cluster ground state, giving rise to a single-molecule magnet. The fact that only shoulders and not peaks are observed for the temperatures and frequencies measured points to a possible quantum tunneling effect, which might be expected from the non-zero *E*-parameter obtained upon fitting the magnetization data.

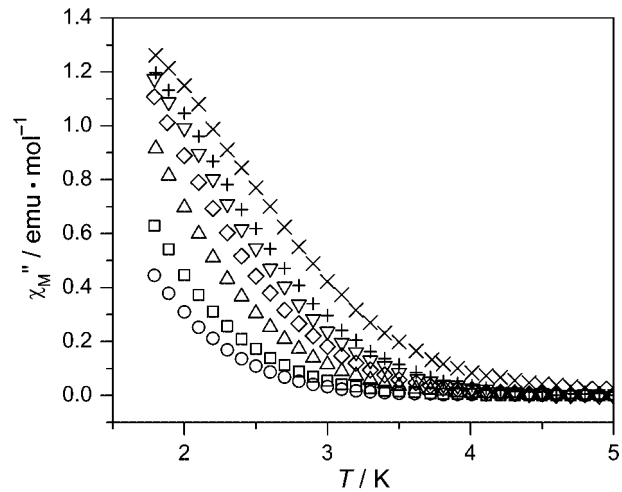

Figure 5 Temperature-dependence of the out-of-phase AC susceptibility for compound **1** recorded at various frequencies − 50 (○), 100 (□), 250 (△), 500 (◇), 750 (▽), 1000 (+), and 1500 (×) Hz.

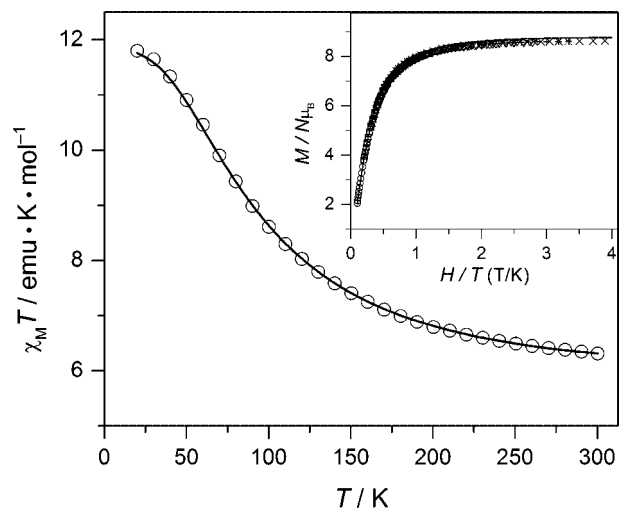

Figure 6 Temperature-dependent magnetic susceptibility data for compound **2β**. The solid line represents the fit to the Heisenberg-van Vleck exchange Hamiltonian described in the text. Inset. Reduced magnetization data for 2β in applied fields of 1-7 T, showing no zero-field splitting. The solid line represents the simulated Brillouin function for an $S = {}^9/_2$ ground state with $g = 2.00$.

The DC magnetic susceptibility for compound **2β** exhibits a room temperature $\chi_M T$ value of 6.31 emu·K/mol, again slightly higher than the expected product of 4.88 emu·K/mol. The observed $\chi_M T$ steadily increases as the temperature is lowered, reaching a maximum of 11.76 emu·K/mol, consistent with a ferromagnetically

coupled $S = {}^9/_2$ ground state, as expected between Cr^{3+} and Cu^{2+}. Fitting the susceptibility data with the spin Hamiltonian given above (M = Cr, M′ = Cu) and MAGFIT 3.1 yielded $J = +20.7\,cm^{-1}$, $g = 1.95$, and TIP = $1640 \times 10^{-6}\,cm^{-1}$. The magnetization data for this compound show superimposable isofield lines, indicating a lack of zero-field splitting in the molecule. As illustrated in the inset of Figure 6, the data closely follow the Brillouin function for an $S = {}^9/_2$ ground state with $g = 2.00$. The magnetic properties of the green unisomerized cluster of compound **2**α are similar to the partially-isomerized isomer, with a slightly reduced exchange constant of $J = +16.9\,cm^{-1}$, and no axial anisotropy (see Figures S1 and S2 in the Supporting Information). An analogous trend was observed for the ferromagnetic exchange coupling in the face-centered cubic cluster $[Tp_8(H_2O)_6Cu_6Cr_8(CN)_{24}]^{4+}$ upon isomerization, but could not be quantified [13b].

Comparison of the magnetic properties of compounds **1** and **2** sheds some light on the effect of single-ion anisotropy in trigonal bipyramidal cyano-bridged clusters. We note that in the previously-reported Cu_3Fe_2 cluster, both magnetic ions, Cu^{2+} and low-spin Fe^{3+}, exhibit single-ion anisotropy due to a first-order Jahn-Teller distortion and first-order orbital angular momentum, respectively. In **1**, the uniaxial anisotropy is dominated by the first-order orbital angular momentum associated with the $^2T_{2g}$ ground term of low-spin Fe^{3+} ions in the axial positions. However, the Ni^{2+} ions in the equatorial plane have no orbital component, as their ground terms are fully symmetric ($^3A_{2g}$ assuming an octahedral crystal field). The Ni_3Fe_2 cluster of **1** shows significant zero-field splitting, albeit smaller in magnitude than the previously reported Cu_3Fe_2 trigonal bipyramid. In turn, the Cu_3Cr_2 cluster of **2** retains the equatorial Cu^{2+} ions with a first-order Jahn-Teller distortion, but the Cr^{3+} ions in the axial positions possess no anisotropy, again due to a fully symmetric ($^4A_{2g}$) ground term. This cluster shows no appreciable anisotropy. Thus, it appears that the single-ion anisotropy from the axial positions, as generated for example by low-spin Fe^{3+}, plays by far the most significant role in controlling the overall molecular anisotropy.

This research was funded by the National Science Foundation (CHE-0617063). We gratefully acknowledge *Dr. C. Crawford* and Unilever for a donation of crude Me_3tacn, *Dr. Anthony T. Iavarone* for assistance with mass spectrometry, *Ms. Ashly M. Hoffman* for fruitful discussions, the University of California President's Postdoctoral Fellowship Program for support of BMB, and the Natural Sciences and Engineering Research Council of Canada for support of MWD.

References

[1] a) R. Sessoli, D. Gatteschi, A. Caneschi, M. A. Novak, *Nature* **1993**, *365*, 141−143; b) R. Sessoli, H. L. Tsai, A. R. Schake, S. Wang, J. B. Vincent, K. Folting, D. Gatteschi, G. Christou, D. N. Hendrickson, *J. Am. Chem. Soc.* **1993**, *115*, 1804−1816.

[2] a) M. N. Leuenberger, D. Loss, *Nature* **2001**, *410*, 789−793; b) J. Tejada, *Polyhedron* **2001**, *20*, 1751−1756; c) J. Tejada, E. M. Chudnovsky, E. del Barco, J. M. Hernandez, T. P. Spiller, *Nanotechnology* **2001**, *12*, 181−186; d) K. M. Mertes, Y. Suzuki, M. P. Sarachik, Y. Myasoedov, H. Shtrikman, E. Zeldov, E. M. Rumberger, D. N. Hendrickson, G. Christou, *Rec. Res. Dev. Phys.* **2003**, *4*, 731−747; e) B. Bernard, *Comptes Rendues Physique* **2005**, *6*, 934−944.

[3] C. J. Milios, A. Vinslava, W. Wernsdorfer, S. Moggach, S. Parsons, S. P. Perlepes, G. Christou, E. K. Brechin, *J. Am. Chem. Soc.* **2007**, *129*, 2754−2755.

[4] A. M. Ako, I. J. Hewitt, V. Mereacre, R. Clérac, W. Wernsdorfer, C. E. Anson, A. K. Powell, *Angew. Chem.* **2006**, *118*, 5048−5051; *Angew. Chem. Int. Ed.* **2006**, *45*, 4926−4929.

[5] L. M. C. Beltran, J. R. Long, *Acc. Chem. Res.* **2005**, *38*, 325−334.

[6] a) K. Van Langenberg, S. R. Batten, K. J. Berry, D. C. R. Hockless, B. Moubaraki, K. S. Murray, *Inorg. Chem.* **1997**, *36*, 5006−5015; b) K. Van Langenberg, D. C. R. Hockless, B. Moubaraki, K. S. Murray, *Synth. Met.* **2001**, *122*, 573−580; c) X.-Y. Chen, W. Shi, J. Xia, P. Cheng, B. Zhao, H.-B. Song, H.-G. Wang, S.-P. Yan, D.-Z. Liao, Z.-H. Jiang, *Inorg. Chem.* **2005**, *44*, 4263−4269; d) C. P. Berlinguette, A. Dragulescu-Andrasi, A. Sieber, H.-U. Güdel, C. Achim, K. R. Dunbar, *J. Am. Chem. Soc.* **2005**, *127*, 6766−6779; e) Z.-G. Gu, Q.-F. Yang, W. Liu, Y. Song, Y.-Z. Li, J.-L. Zuo, X.-Z. You, *Inorg. Chem.* **2006**, *45*, 8895−8901; f) M. Shatruk, K. E. Chambers, A. V. Prosvirin, K. R. Dunbar, *Inorg. Chem.* **2007**, *46*, ASAP.

[7] C.-F. Wang, J.-L. Zuo, B. M. Bartlett, Y. Song, J. R. Long, X.-Z. You, *J. Am. Chem. Soc.* **2006**, *128*, 7162−7163.

[8] R. Lescouëzec, J. Vaissermann, F. Lloret, M. Julve, M. Verdaguer, *Inorg. Chem.* **2002**, *41*, 5943−5945.

[9] M. P. Shores, P. A. Berseth, J. R. Long, *Inorg. Syn.* **2004**, *34*, 149−155.

[10] F. H. Fry, A. J. Fischmann, M. J. Belousoff, L. Spiccia, J. Brügger, *Inorg. Chem.* **2005**, *44*, 941−950.

[11] J. H. Coates, D. A. Hadi, S. F. Lincoln, H. W. Dodgen, J. P. Hunt, *Inorg. Chem.* **1981**, *20*, 707−711.

[12] a) D. F. Shriver, S. A. Shriver, S. E. Anderson, *Inorg. Chem.* **1965**, *4*, 725−730; b) D. B. Brown, D. F. Shriver, L. H. Schwartz, *Inorg. Chem.* **1968**, *7*, 77−83; c) D. B. Brown, D. F. Shriver, *Inorg. Chem.* **1969**, *8*, 37−42; d) J. E. House, Jr., J. C. Bailar, Jr., *Inorg. Chem.* **1969**, *8*, 672−673; e) E. Reguera, J. F. Bertrán, L. Nuñez, *Polyhedron* **1994**, *13*, 1619−1624; f) R. Martínez-Garcia, M. Knobel, E. Reguera, *J. Phys. Chem. B* **2006**, *110*, 7296−7303.

[13] a) B. S. Lim, R. H. Holm, *Inorg. Chem.* **1998**, *37*, 4898−4908 and references therein; b) T. D. Harris, J. R. Long, *Chem. Commun.* **2007**, 1360−1362.

[14] E. A. Schmitt. *Characterization of Tetranuclear Manganese Complexes and Thermochromic Cu(II) and Ni(II) Complexes.* University of Illinois Urbana-Champaign, 1997.

[15] M. P. Shores, J. J. Sokol, J. R. Long, *J. Am. Chem. Soc.* **2002**, *124*, 2279−2292.

